AUTOPSY STUDY OF TESTICLES IN COVID-19: UPREGULATION OF IMMUNE-RELATED GENES AND DOWNREGULATION OF TESTIS-SPECIFIC GENES

Alessio Basolo[1], Anello Marcello Poma[2], Elisabetta Macerola[2], Diana Bonuccelli[3], Agnese Proietti[2], Alessandra Salvetti[4], Paola Vignali[2], Liborio Torregrossa[2], Laura Evangelisti[3], Rebecca Sparavelli[2], Riccardo Giannini[2], Clara Ugolini[2], Fulvio Basolo[2], Ferruccio Santini[1], Antonio Toniolo[5]

[1] *Obesity and Lipodystrophy Center, Endocrinology Unit, University Hospital of Pisa, 56124, Pisa, Italy*

[2] *Department of Surgical, Medical, Molecular Pathology and Critical Area, University Hospital of Pisa, Pisa, Italy*

[3] *Department of Forensic Medicine, Azienda USL Toscana Nordovest, Lucca, Italy*

[4] *Department of Clinical and Experimental Medicine, University of Pisa, Pisa, Italy*

[5] *Global Virus Network, University of Insubria, 21100 Varese, Italy.*

Short title: Infection of testis in COVID-19

Key Words: COVID-19, autopsy, testis, SARS-CoV-2, innate immunity, testis-specific genes.

Corresponding author: Alessio Basolo, MD, Obesity and Lipodystrophy Center, Endocrinology Unit, University Hospital of Pisa, 56124, Pisa, Italy

Telephone number: +39-050-997334

ORCID ID: 0000-0001-6888-7080

Authors' last names: Basolo A., Poma, Macerola, Bonuccelli, Proietti, Salvetti, Vignali, Torregrossa, Evangelisti, Sparavelli, Giannini, Ugolini, Basolo F., Santini, Toniolo

E-mail addresses: alessio.basolo@med.unipi.it; marcellopoma@gmail.com; elisabetta.macerola@for.unipi.it; diana.bonuccelli@uslnordovest.toscana.it; agneseproietti@gmail.com; alessandra.salvetti@unipi.it; paola.vignali@phd.unipi.it; libo.torregrossa@gmail.com; laura.evangelisti@uslnordovest.toscana.it; r.sparavelli@studenti.unipi.it; riccardo.giannini@dc.unipi.it; clara.ugolini@gmail.com; fulvio.basolo@med.unipi.it; ferruccio.santini@med.unipi.it; antonio.toniolo@gmail.com

Disclosure statement

The authors declare no conflict of interest.

Abbreviations: FFPE, Formalin-fixed and paraffin-embedded; BMI, body mass index (weight in kilograms divided by the square of height in meters); IFN, Interferon; ACE2, Angiotensin-Converting Enzyme-2; TMPRSS2, transmembrane serine protease 2.

Abstract

Context. Infection by SARS-CoV-2 may be associated with testicular dysfunction that could affect male fertility.

Objective. Testicles of fatal COVID-19 cases were investigated to detect virus in tissue and to evaluate histopathological and transcriptomic changes.

Methods. Three groups were compared: a. uninfected controls (subjects dying of trauma or sudden cardiac death; n=10); b. subjects dying of COVID-19 (virus-negative in testes; n=15); c. subjects dying of COVID-19 (virus-positive in testes; n=9). SARS-CoV-2 genome and nucleocapsid antigen were probed using RT-PCR, in situ hybridization, immunohistochemistry (IHC). Infiltrating leukocytes were typed by IHC. mRNA transcripts of immune-related and testis-specific genes were quantified using the nCounter method.

Results. SARS-CoV-2 was detected in testis tissue of 9/24 (37%) COVID-19 cases accompanied by scattered T-cell and macrophage infiltrates. Size of testicles and counts of spermatogenic cells were not significantly different among groups. Analysis of mRNA transcripts showed that in virus-positive testes immune processes were activated (interferon-alpha and -gamma pathways). By contrast, transcription of 12 testis-specific genes was downregulated, independently of virus positivity in tissue. By IHC, expression of the luteinizing hormone/choriogonadotropin receptor was enhanced in virus-positive compared to virus-negative testicles, while expression of receptors for androgens and the follicle-stimulating hormone were not significantly different among groups.

Conclusion. In lethal COVID-19 cases, infection of testicular cells is not uncommon. Viral infection associates with activation of interferon pathways and downregulation of testis-specific genes involved in spermatogenesis. Due to the exceedingly high numbers of infected people in the pandemic, the impact of virus on fertility should be further investigated.

Introduction

The pandemic caused by the Severe Acute Respiratory Syndrome Coronavirus-2 (SARS-CoV-2) produced more than 600 million infections and about 6.5 million deaths worldwide (last accessed: September 03, 2022, https://coronavirus.jhu.edu/map.html). Previous work demonstrated that the responsible virus may target endocrine organs such as the adrenals [1, 2], thyroid [3, 4], ovaries [5], pancreatic islets [6-8], pituitary [1, 9-11] and adipose tissue [12]. In autoptic specimens of COVID-19 subjects, the virus has been detected in a variety of endocrine cells and, possibly, is linked with endocrine dysfunctions [13-15]. The virus has also been detected in semen suggesting that fertility is affected [16, 17]. The tropism of SARS-CoV-2 is governed by the expression of multiple cell entry factors [18]. It is plausible that SARS-CoV-2 enters cells of the male reproductive tract through the angiotensin-converting enzyme 2 (ACE2)/transmembrane serine protease 2 (TMPRSS2) pathway [19]. In fact, autopsy studies of lethal COVID-19 cases showed high-levels of ACE2 and TMPRSS2 mRNA transcripts in testicles, while moderate TMPRSS2 staining was observed in glandular cells of the prostate [20]. Single-cell RNA sequencing of testicular cells showed that ACE2 is highly transcribed in Sertoli cells, Leydig cells and spermatogonia [21] in addition to myoid, stromal, and spermatogonial stem cells [22]. In contrast, the expression of TMPRSS2 seems limited to spermatogonial stem cells, spermatogonia, spermatocytes and spermatids [22]. Thus, it appears that SARS-CoV-2 entry factors are widely expressed in testicular cells. However, a functional blood-testis barrier – whose task is to protect the reproductive cells from autoimmune attacks and infectious agents [23, 24] – is expected to hinder the penetration of viruses into testes.

Interestingly, it has been shown in multiple organs that ACE2 and TMPRSS2 are expressed at higher levels in men than in women, suggesting a sex-centered bias in virus susceptibility [25]. It has also been proposed that immune-mediated pathology may contribute to damage of testicles in COVID-19 and to reduce the semen index [26]. Though infection of the male genital tract is a possible event during

COVID-19, two studies failed to detect the virus in testicles [16, 27] while one study detected the virus in testicles of two COVID-19 cases using both RT-PCR and immunohistochemistry [28]. At autopsy, virus particles were observed in the interstitial compartment of testicles suggesting an indirect impairment of spermatogenesis [28].

Likewise, clinical reports indicate that COVID-19 cases may associate with a reduction of sex hormone levels [i.e., testosterone (T), follicle-stimulating hormone (FSH), luteinizing hormone (LH)], suggesting a dysfunction of the hypothalamic–pituitary–gonadal (HPG) axis [29, 30]. Published post mortem studies have demonstrated age-related changes in daily sperm production and testicular weights[31] and that the efficacy of hormonal methods to suppress spermatogenesis varies across ethnic groups[32]. Our study of fatal COVID-19 cases aimed at detecting SARS-CoV-2 in testicle specimens and at evaluating histopathological changes and inflammatory infiltrates. In addition, levels of mRNA transcripts of immune-related genes and testis-specific genes were quantified to check whether infection were associated with dysfunctional changes in gene expression of testicular cells.

Materials and methods

Investigated COVID-19 cases and controls

As shown in **Table 1**, three case groups have been investigated: a) controls, i.e. subjects who died abruptly from non-infectious causes (trauma, sudden cardiac death; n=10); b) subjects dying from COVID-19 (SARS-CoV-2-negative in testes; n=15); c) subjects dying from COVID-19 (SARS-CoV-2-positive in testes; n=9). The investigated subjects were of Caucasian ethnicity. Autopsies have been performed in a BSL3 facility [33] at the Unit of Forensic Medicine (Azienda USL Toscana Nord Ovest, Lucca, Italy) that serving four major Hospitals: Pisa, Lucca, Livorno and Massa-Carrara. The three groups were comparable with regard to comorbidities. The current observational study was approved by the local Ethics Committee (Comitato Etico Area Vasta Nord-Ovest, Italy No. 17327, 2020-05-14).

All cases were screened for the SARS-CoV-2 genome in both lungs as well as in testis tissue. As previously reported[3], the virus and alterations of lung parenchyma consistent with moderate to severe disease were detected in all COVID-19 cases, not in controls. For histology, virus detection and analysis of mRNA transcripts, two tissue specimens (surface area of about 1.5 cm^2) were taken as representing the entire testis. Specimens of COVID-19 cases were compared to those of uninfected controls regarding histopathological features and infiltrating leukocytes, detection of SARS-CoV-2 genome and antigens, transcription levels of immune-related and testis-specific genes. Histopathology of testis tissue of a SARS-CoV-2-positive case is shown in **Figure 1A**.

Histopathology and immunohistochemistry (IHC)

Three-μm-thick sections were used for immunohistochemistry (IHC). For viral antigens, a SARS-CoV-2 nucleocapsid antibody was used (NB100-56683, Novus Biologicals, Centennial, CO, USA, RRID: AB_838841). In addition, expression of the following immune cell markers (CONFIRM series, Ventana Medical Systems, AZ, USA) was evaluated: anti-CD20 (B-cell marker clone L26; RRID AB_2335956), anti-CD3 (T-cell marker clone 2GV6; RRID AB_2335978), anti-CD45, LCA (pan-leukocyte marker clone RP2/18; RRID AB_2335953), anti-CD57 (natural killer, NK cell marker clone NK1; RRID AB_2920583), anti-CD68 (macrophage marker, clone KP-1; RRID AB_2335972), anti-CD8 (cytotoxic T-cell marker, clone SP57; RRID AB_2335985). Slides were counterstained with hematoxylin and bluing reagent. The IHC staining for immune cell markers was evaluated in ten randomly selected 40x fields, and mean counts were compared among groups. IHC detection of the androgen receptor (AR), follicle stimulating hormone Receptor (FSHR), luteinizing hormone/choriogonadotropin receptor (LHCGR) was performed with the following antibodies: AR rabbit mAb 760-4605 (Ventana Medical Systems; RRID AB_2921271); FSHR mouse mAb 6E8.2F5 (Novus Biologicals; RRID AB_2895285); LHR rabbit polyclonal antibody NLS1436 (Novus

Biologicals; RRID AB_10001001). The percentage of AR and FSHR in seminiferous tubuli is reported together with that of LHCGR in extra-tubular cells.

Testicles size and evaluation of germ cells in seminiferous tubuli

For each case, testicular length and width in centimeters was measured with a ruler and noted, but the side of the body of the measured testis was not recorded. For each case, spermatogenic populations were typed and counted in H&E slides at 40x. In each section, 40-70 tubules were observed. Spermatogonia, spermatocytes, and spermatids were counted. Spermatogonia lie in the basal compartment of adult testes. Their nuclei are oval to round and have one or two easily identifiable nucleoli. Primary spermatocytes and secondary spermatocytes have not been distinguished from each other but evaluated as a single category. Their nuclei are larger than those of spermatogonia with finely granular chromatin. Secondary spermatocytes undergo the second meiotic division to produce spermatids. Spermatids have been considered as a single category, though the classification of Heller-Clermont differentiates six types [34]. The late spermatid forms are characterized by a change in the nuclear shape to an oval contour, then to an elongated appearance and a marked condensation of chromatin. Well preserved spermatozoa could not be clearly detected in the analyzed slides.

Detection of SARS-CoV-2 genome and transcripts by RT-PCR and by in situ hybridization

RNA was isolated from two to three 10 µm-thick sections by the RNeasy FFPE kit (Qiagen, Hilden, Germany). RNA was quantified using an Xpose spectrophotometer (Trinean, Gentbrugge, Belgium). The Easy SARS-CoV-2 WE kit (Diatech Pharmacogenetics, Jesi, Italy) was used to detect the virus genome in lung and testis specimens. For each assay, about 250 ng of RNA were utilized. According to the manufacturer’s instructions, specimens were deemed virus-positive when the nucleocapsid (N) gene was amplified before the 36th cycle threshold (Ct) and/or the RNA-dependent RNA polymerase (RdRp) gene was amplified before the 38th Ct.

In situ hybridization (ISH) was performed using the RNAscope Probe V-nCoV2019-S (Advanced Cell Diagnostics, Bio-Techne, Minneapolis, MN, USA) and the RNAscope Intro Pack 2.5 HD Reagent Kit Brown for manual assays. The probe targets the SARS-CoV-2 spike (S) gene and was designed on the original Wuhan-Hu-1 sequence (NC_045512.2). Positive and negative control probes target the human peptidylprolyl isomerase B (*PPIB*) gene and the bacterial dapB gene of Bacillus subtilis, respectively. Unstained 4 µm-thick sections were incubated with target retrieval reagents at 100°C for 15 minutes. Washing steps and treatment with proteases at 40°C for 30 minutes were performed followed by probe hybridization. Detection was carried out by DAB staining. Slides were counterstained with hematoxylin.

Transmission electron microscopy

Small pieces of testis tissue (approximately 1 mm^3) were fixed with 2.5% glutaraldehyde in 100 mM sodium cacodylate buffer for 3 hours at 4°C and processed for transmission electron microscopy [35]. Samples were post-fixed in 1% osmium tetroxide for 1 hour, dehydrated in graded series of ethanol solutions and embedded in Epon Araldite resin. Ultrathin sections were stained with uranyl acetate and lead citrate and analyzed with a Jeol 100 SX transmission electron microscope (Jeol, Tokyo, Japan). Digital images and measurements were acquired using an AMT image capture software (AMT, Woburn, MA, USA).

Transcription levels of virus-specific, immune-related and testis-specific genes as measured by the nCounter method nCounter assays (nanoString Technologies, Seattle, WA, USA) were performed using 175 ng of RNA per assay. Hybridization was carried out at 65°C for 21 hours. Three probe panels were used: A) the Coronavirus Panel Plus that includes 9 probes targeting the SARS-CoV-2 virus, 1 probe for the human gene encoding ACE2, and probes targeting the N and S ORFs of coronaviruses other than SARS-CoV-2 (HCoV-229E, HCoV-HKU1, HCoV-NL63, HCoV-OC43, and SARS-CoV). Probes for SARS-CoV-2 were designed on the reference sequence Wuhan-Hu-1 (NC_045512); B) the Human Host Response panel that includes 773 genes covering the host immune response to infectious diseases, plus 12 internal reference housekeeping genes for data normalization; C) a custom panel that contains 10 housekeeping genes and 12 testis-specific genes: *ACTL7B* (testis tissue sperm-binding protein li 43a); *ADAD1* (testis-specific adenosine deaminase domain containing 1 that plays a role in spermatogenesis); *ADAM2* (ADAM metallopeptidase domain 2, a sperm surface membrane protein involved in sperm-egg plasma membrane adhesion and fusion during fertilization); *CCDC70* (coiled-coil domain-containing protein 70 in plasma membrane); *H2AC1* (H2A clustered histone 1 that plays a role in transcription regulation, DNA repair, DNA replication and chromosomal stability); *H2BC1* (H2B clustered histone 1, a variant histone required to direct the transformation of dissociating nucleosomes to protamine in male germ cells); *HMGB4* (high mobility group box 4, a nuclear protein regulating transcription by RNA polymerase II); *LYZL1* (lysozyme-like protein 1 located in the extracellular region); *SLC25A31* (solute carrier family 25 member 31 that exchanges cytosolic ADP for matrix ATP in mitochondria and is required in spermatocytes); *SUN5* (sperm-associated antigen 4-like protein that plays a role in the meiotic stage of spermatogenesis anchoring sperm head to the tail); *TEX33* (testis-expressed protein 33 that is found in the cytoplasm of round spermatids but less in elongated spermatids); *TUBA3C* (tubulin alpha 3c, a major constituent of microtubules). The choice of testis-specific genes was based on The Human Protein Atlas (https://www.proteinatlas.org/). The top testis tissue-enriched genes were selected, while genes expressed also in other tissues were filtered out.

Data analyses

Raw gene expression counts were normalized using the Advanced Analysis module of the nSolver software v.4.0 (nanoString Technologies) after filtering out low-count genes. Normalized counts were log2-transformed. To compute differentially expressed genes (DEG), controls were used as baseline and were contrasted against virus-positive and virus-negative testis samples of the COVID-19 group. Age was used as confounder and *p*-values were adjusted by the Benjamini-Hochberg method. DEG analysis was performed following the procedures of the Advanced Analysis module in the nSolver software. A false discovery rate (FDR) below 0.05 was considered significant. The ranked gene lists were then used for Gene Set Enrichment Analysis (GSEA) following the procedures of the clusterProfiler Bioconductor package v.4.2.0. The Hallmark (H) and Gene Ontology (C5) collections from the Mutational Signatures Database (MutSigDB) v.7.4 were used as reference. IHC scores were compared by ANOVA using age as confounder followed by Tukey's test. With the exception of gene expression normalization and DEG computing, all analyses were performed in the R environment v.4.1.2 (https://www.r-project.org/, last accessed March 14, 2022).

Results

Detection of SARS-CoV-2 in testicles

By real-time RT-PCR, the SARS-CoV-2 genome was detected in 9/24 (37%) testis specimens from COVID-19 cases. Only four of the latter cases showed detectable amounts of SARS-CoV-2 transcripts using the nCounter assay (hybridization assay without gene amplification). These findings show that the majority of COVID-19 cases had low viral loads in testis tissue. None of the controls was virus-positive by either RT-PCR or the nCounter assay. SARS-CoV-2 positivity by real-time RT-PCR was confirmed by IHC staining for the nucleocapsid antigen and of ISH for the visualization of the viral genome (**Figure 1B and 1C**). In a few samples, the presence of SARS-CoV-2 was confirmed by electron microscopy that showed enveloped virus-like particles (approximately 100nm in diameter) and faint projections on the surface (**Figure 2**). Virus-like particles were located in the cytoplasm within membrane-bounded vesicles.

Size of testicles and evaluation of germ cells in seminiferous tubuli

As shown in **Table 2**, the length and width of testicles at autopsy were not significantly different among the investigated groups. Similarly - as assessed in H&E slides - the counts of spermatogonia, spermatocytes and spermatids were not significantly different among groups. Possibly related to the slightly greater mean age of COVID-19 groups compared to uninfected controls, the size of testicles and the numbers of spermatogenic cells tended to be slightly - but not significantly - lower in the two COVID-19 groups.

Histopathology and inflammatory infiltrates in testes of COVID-19 cases and controls

No differences in histopathological features were observed between COVID-19 subjects and controls, but inflammatory cell infiltrates were more represented in the COVID-19 cohort compared to controls independently of virus presence in testis tissue. CD3 and CD8-positive T-cell infiltrates were scattered among seminiferous tubuli (**Figure 1D**), while clusters of CD68 macrophages were found in the extra-tubular space (**Figure 1E**). CD20 B cells and CD57 NK cells were absent or extremely rare. Due to the large intra-group variation, no significant differences were found between cases that were SARS-CoV-2 positive or negative in testis tissue.

Transcripts of immune-related genes in testicles of COVID-19 subjects as measured by the nCounter method

Gene expression analysis in testes of subjects dying of COVID-19 showed a predominant upregulation of immune genes independently of virus detection in the testes. However, gene expression changes were not statistically significant after multiple comparison correction due to relatively low sample size, overall small fold changes and high standard errors demonstrating a high intra-group variability. Remarkably, transcript levels of the ACE2 gene were not significantly different between COVID-19 cases and controls (FDR=0.99 and FDR=0.47 in virus-positive and virus-negative COVID-19 cases, respectively). As shown in **Table 3**, only one gene, the interferon alpha inducible protein 6 (*IFI6*) – that is endowed with antiviral activity and negatively regulates the intrinsic apoptotic pathway – was strongly upregulated in virus-positive testicles compared to controls (FDR=0.001). A trend to enhanced transcription was also seen for the *ISG15* and *MARCO* genes. *ISG15*, a ubiquitin-like protein, binds intracellular target proteins upon activation by type I interferons. *MARCO* (macrophage receptor with collagenous structure) is part of the innate antimicrobial immune system.

Significantly deregulated gene pathways in the two COVID-19 groups versus the control group

To identify possible alterations of immune pathways, a Gene Set Enrichment Analysis (GSEA) was performed. The deregulated gene pathways are summarized in **Table 4**. Interestingly, in virus-positive testicles numerous immune processes were significantly enhanced, including the interferon-gamma and alpha response, the TNF-alpha signaling via NFkB, the complement pathway and the inflammatory response. The latter processes were activated with FDR values ranging from 0.000006 to 0.04. Conversely, in virus-negative testicles only two immune processes were significantly activated: the inflammatory response and the allograft rejection pathway (FDR 0.02 and 0.03, respectively).

Transcription levels of testis-specific genes in testicles of COVID-19 subjects as measured by the nCounter method

As compared to uninfected controls who died abruptly of trauma or sudden cardiac death, the transcripts of 12 testis-specific genes were downregulated in testicles of COVID-19 cases (both virus-positive and virus-negative). However, statistical significance was not reached due to the relatively low numbers of investigated cases and the high intra-group variability. Data are presented in **Table 3.** Downregulation was more pronounced for *SLC25A31* that is expressed in spermatocytes, *TEX33* that is specific of round spermatids, *TUBA3C* a major constituent of microtubules, *ADAD1* that is required for male fertility and normal male germ cell differentiation.

Correlation of inflammatory infiltrates with transcription levels of testis-specific genes

Aging, ethnicity and chronic illness are independent in their effects on testicular size and function [32, 36]. In the investigated subjects, the macroscopic appearance and cellular composition of testicular tissue was not markedly different between COVID-19 cases and controls, with the exception of modest inflammatory infiltrates in the virus-infected group. Thus, in analyzing transcript levels of testis-specific genes, the effects of age and BMI as potential confounders were subtracted. The correlation of testis-specific gene transcripts with the abundance of different types of infiltrating immune cells (CD45, CD3, CD8, CD68) was also evaluated. As shown in **Figure 3**, immune cell counts were positively correlated among themselves. The same was true for transcripts levels of testis-specific genes. In contrast, levels of infiltrating immune cells were negatively related to selected testis-specific transcripts (*ADAD1*, *ADAM2*, *H2AC1*, *H2BC1*, *SLC25A31*, *TUBA3C*). Interestingly, transcription of genes mostly expressed in spermatidis (*ACTL7B*, *CCDC70*, *HMGB4*, *LYZL1*, *SUN5*, *TEX33*) was reduced but not related to immune cell counts.

Though the reduced transcription of some testis genes may be explained - at least in part - by the presence of immune infiltrates, the transcription of spermatids-specific genes was suppressed independently of the presence of inflammatory cells. Of note, counts of spermatogenic cells were not significantly different among the investigated groups (two COVID-19 groups and uninfected controls).

Immunohistochemical evaluation of sex hormone receptors in testis sections

The expression of the AR, FSHR and LHCGR was evaluated by immunohistochemistry in testis sections (**Figure 1F, G, H**). **Figure 4** shows a quantitative analysis of IHC results. Though statistical significance was not reached, a trend to enhanced expression levels of AR was observed in COVID-19 cases (15.1% and 18.6% on average in virus-positive and virus-negative cases respectively) compared to controls (5.6%). Similarly, statistically significant differences were not observed in FSHR expression levels though a trend to reduction was present for FSRH in testes of COVID-19 cases (25.7% in virus-positive and 37.1% in virus-negative) compared to controls (47.5%). By contrast, expression of LHGCR was significantly enhanced in virus-positive testes (21.6%) compared to both virus-negative testes (6.7%, p=0.05) and to uninfected controls (3.7%, p=0.03).

Discussion

Infection by SARS-CoV-2 may be associated with testicular dysfunction [20, 22]. Since the virus entry factors ACE2 and TMPRSS2 are expressed in testicular cells [20, 22, 37], SARS-CoV-2 infection has the potential for damaging somatic and germline cells [38]. In our study of lethal COVID-19 cases, RT-PCR assays could detect the SARS-CoV-2 genome in testicles of about one third of cases. In virus-positive cases, staining for the nucleocapsid antigen and ISH for detecting the viral genome confirmed the presence of virus in cells of the extra-tubular space (possibly Leydig cells) and in cells of seminiferous tubuli, i.e. cells involved in the production of gametes. The presence of virus-like particles in sections of testicle tissue was also confirmed by electron microscopy, but the type of virus-infected cells was difficult to identify. Notably, no major histopathological changes were observed in testicles of COVID-19 cases, suggesting the apparent lack of morphologically detectable tissue damage. Importantly, cases that were virus-positive in testes showed a significantly shorter mean time from initial symptoms to death compared to cases that were virus-negative in the organ, suggesting that the presence of virus was associated with the more severe or more acute forms of infection.

Moderate infiltrates of T-lymphocytes and macrophages were detected in testicles of COVID-19 cases. Our findings are in line with a report of Ma and collaborators [28] who investigated the possible alterations of spermatogenesis in severe COVID-19 cases. The study of Ma et al. [28] showed that SARS-CoV-2 antigens are expressed in cells of seminiferous tubuli as well as in cells of the extra-tubular space. This report also showed that the ACE2 and TMPRSS2 entry factors are expressed more intensely in testicular sections of COVID-19 cases as compared to uninfected controls [28]. Notably, the expression of ACE2 has been shown to be enhanced in subjects with obesity [39] and is also potentiated by androgens [17]. In the course of SARS-CoV-2 infection, some cases of hypogonadism and reduced levels of testosterone have been reported [17, 30]. These could be related to hypofunctional Leydig cells that produce testosterone [40, 41]. It is known that testicle functions are regulated by pituitary hormones, notably by FSH and LH. For this reason, tissue sections were evaluated by IHC to assess the expression levels of reproductive hormone receptors. Though not significantly different among groups, the percentage of AR-positive cells in seminiferous tubuli tended to be higher in COVID-19 cases compared to controls, while the percentage of FSHR-positive cells was reduced in seminiferous tubuli. Interestingly, the percentage of LHCGR-positive extra-tubular cells was significantly higher in tissue of subjects that were virus-positive in testes compared to those that were virus-negative in testes and to uninfected controls. The significance of the enhanced expression of LHCGR in virus-containing testes remains unclear. Based on previous observations of pituitary tissue in COVID-19 cases[42], the upregulation of LHCGR in SARS-CoV-2-positive testes may be related to a feedback adaptation to reduced circulating levels of LH.

Transcription analysis of immune-related genes showed the upregulation of three genes of the innate antiviral immunity: *IFI6*, *ISG15* and *MARCO*. The IFI6 protein protects uninfected cells by preventing the formation of virus-induced endoplasmic reticulum membrane invaginations that are needed for virus replication [43]. This IFN-stimulated gene is active against a variety of agents, including SARS-CoV-2 and Zika virus [44]. ISG15 contributes to activate the melanoma differentiation-associated protein 5 (MDA5), a key sensor of viral nucleic acids. Notably, SARS-CoV-2 antagonizes this gene product through a virus-coded protease [45, 46]. Finally, type I IFNs also upregulate the scavenger macrophage receptor MARCO that plays multiple roles in innate immunity [47].

Activation of the IFN response in testes of COVID-19 patients was confirmed by GSEA that showed a significant upregulation of the IFN-alpha and IFN-gamma responses. This corroborates our previous findings in autopsy cases of COVID-19 regarding other endocrine organs and confirmed that IFN-mediated defenses are essential for the antiviral protection of endocrine tissues [3, 15, 42, 48, 49].

Notably, the size of testicles and the counts of spermatogenic cells in seminiferous tubuli were not significantly different among the investigated groups. However, testis-specific transcripts tended to be downregulated in COVID-19 cases compared to controls, independently of virus detection within testicles. Though the high intra-group variation and the small number of investigated cases did not allow to reach statistical significance for individual genes, downregulation of an entire set of genes indicates that infection by SARS-CoV-2 contributes to reducing testicular functions through a direct effect of virus on testicular cells and, possibly, as bystander effect of inflammatory and immune processes [22]. The finding that counts of infiltrating immune cells were negatively correlated to selected testis-specific transcripts may also be explained by the "dilution effect" of infiltrating immune cells in testicle tissue, and/or by the suppression of transcription brought about by activation of the IFN system in the context of a local inflammatory infiltrate [50]. The suppressed transcription of spermatids-specific genes was, however, independent of immune cell infiltrates. In the case of mumps virus, which is well known for affecting male fertility, the ability of the virus to disrupt the blood-testis barrier has been demonstrated [51]. More recently, it has been shown that emerging pathogens such as Zika, Lassa, Ebola and Marburg viruses can infect testes in humans and affect fertility [52]. The same should be taken into consideration for SARS-CoV-2.

Our observational study has some limitations: a) small numbers of cases have been analyzed in each group; b) autoptic specimens usually refer to patients with severe infection, which may not reflect the conditions proper of mild to moderate cases; c) the times before death varied among cases; d) serum reproductive hormones were not measured e) autopsy and tissue collection were mostly performed days after death, thus tissue morphology may be not well preserved; f) the SARS-CoV-2 variants responsible of the investigated cases were not ascertained.

In conclusion, the findings show that the presence of SARS-CoV-2 in testicles is associated with activation of IFN pathways and with the downregulation of testis-specific genes that play a role in spermatogenesis. Due to the exceedingly high number of people infected in the course of the pandemic, SARS-CoV-2 could greatly impact fertility. Preventive and therapeutic measures that may limit the impact of virus on human reproduction are encouraged.

Acknowledgments

The study has been conducted in collaboration with the Global Virus Network (GVN), Baltimore, MD and the Centro Linceo Beniamino Segre, Accademia dei Lincei, Rome, Italy.

Author Contributions

Conceptualization, A.B., A.T., F.B., A.M.P., F.S.; clinical work and autopsy samples: D.B., A.B.; F.C., F.B.; methodology, A.B., A.M.P., F.B., A.T., A.P., E.M., C.U., L.T., L.E., R.S., R.G., P.V., A.S.;

formal analysis, A.B., A.T., A.M.P., D.B.; resources, F.B., A.T.; preparation of the original draft, A.B., A.T., F.B., A.M.P.; writing, review and editing, A.T., A.B., F.B., A.M.P., F.S., L.T.; project administration, F.B., A.T.; funding acquisition, F.B., A.T. All authors have read, revised and approved the final version of the manuscript.

Disclosure statement

The authors declare no conflict of interest.

Funding

The study was funded by: Tuscany Region (PRE-MED2, Progetto Salute 2018 to F.B.), the Juvenile Diabetes Research Foundation & nPOD-V (JDRF grant 25-2012-770 to AT), the Italian Ministry of Health (grant PE-2013-02357094 to A.T.).

Ethical approval

The study has been approved by the local Ethical Committee (Comitato Etico Area Vasta Nord-Ovest, Lucca, Italy No. 17327, 2020-05-14). The procedures employed in the study are in accordance with the ethical standards of the Local Ethical Committee and with the 1964 Helsinki Declaration and its later amendments.

Data availability:

Some or all datasets generated during and/or analyzed during the current study are not publicly available but are available from the corresponding author on reasonable request.

References

1. Alzahrani AS, Mukhtar N, Aljomaiah A, Aljamei H, Bakhsh A, Alsudani N, Elsayed T, Alrashidi N, Fadel R, Alqahtani E, Raef H, Butt MI, Sulaiman O. The Impact of COVID-19 Viral Infection on the Hypothalamic-Pituitary-Adrenal Axis. *Endocr Pract*. Feb 2021;27(2):83-89. doi:10.1016/j.eprac.2020.10.014
2. Kanczkowski W, Evert K, Stadtmüller M, Haberecker M, Laks L, Chen LS, Frontzek K, Pablik J, Hantel C, Beuschlein F, Kurth T, Gruber S, Aguzzi A, Varga Z, Bornstein SR. COVID-19 targets human adrenal glands. *Lancet Diabetes Endocrinol*. Jan 2022;10(1):13-16. doi:10.1016/s2213-8587(21)00291-6
3. Poma AM, Basolo A, Bonuccelli D, Proietti A, Macerola E, Ugolini C, Torregrossa L, Alì G, Giannini R, Vignali P, Santini F, Toniolo A, Basolo F. Activation of Type I and Type II Interferon signaling in SARS-CoV-2-positive thyroid tissue of patients dying from COVID-19. *Thyroid*. Sep 19 2021;doi:10.1089/thy.2021.0345
4. Speer G, Somogyi P. Thyroid complications of SARS and coronavirus disease 2019 (COVID-19). *Endocr J*. Feb 28 2021;68(2):129-136. doi:10.1507/endocrj.EJ20-0443
5. Wong DWL, Klinkhammer BM, Djudjaj S, Villwock S, Timm MC, Buhl EM, Wucherpfennig S, Cacchi C, Braunschweig T, Knüchel-Clarke R, Jonigk D, Werlein C, Bülow RD, Dahl E, von Stillfried S, Boor P. Multisystemic Cellular Tropism of SARS-CoV-2 in Autopsies of COVID-19 Patients. *Cells*. Jul 27 2021;10(8)doi:10.3390/cells10081900
6. Müller JA, Groß R, Conzelmann C, Krüger J, Merle U, Steinhart J, Weil T, Koepke L, Bozzo CP, Read C, Fois G, Eiseler T, Gehrmann J, van Vuuren J, Wessbecher IM, Frick M, Costa IG, Breunig M, Grüner B, Peters L, Schuster M, Liebau S, Seufferlein T, Stenger S, Stenzinger A, MacDonald PE, Kirchhoff F, Sparrer KMJ, Walther P, Lickert H, Barth TFE, Wagner M, Münch J, Heller S, Kleger A. SARS-CoV-2 infects and replicates in cells of the human endocrine and exocrine pancreas. *Nat Metab*. Feb 2021;3(2):149-165. doi:10.1038/s42255-021-00347-1
7. Wu CT, Lidsky PV, Xiao Y, Lee IT, Cheng R, Nakayama T, Jiang S, Demeter J, Bevacqua RJ, Chang CA, Whitener RL, Stalder AK, Zhu B, Chen H, Goltsev Y, Tzankov A, Nayak JV, Nolan GP, Matter MS, Andino R, Jackson PK. SARS-CoV-2 infects human pancreatic β cells and elicits β cell impairment. *Cell Metab*. Aug 3 2021;33(8):1565-1576.e5. doi:10.1016/j.cmet.2021.05.013
8. Mine K, Nagafuchi S, Mori H, Takahashi H, Anzai K. SARS-CoV-2 Infection and Pancreatic β Cell Failure. *Biology (Basel)*. Dec 24 2021;11(1)doi:10.3390/biology11010022
9. Ilera V, Delfino LC, Zunino A, Glikman P, Drnovsek M, Reyes A, Dios A, Toibaro J, Pachioli V, Lannes N, Guida A, Gauna A. Correlation between inflammatory parameters and pituitary-thyroid axis in patients with COVID-19. *Endocrine*. Dec 2021;74(3):455-460. doi:10.1007/s12020-021-02863-2
10. Misgar RA, Rasool A, Wani AI, Bashir MI. Central diabetes insipidus (Infundibuloneuro hypophysitis): A late complication of COVID-19 infection. *J Endocrinol Invest*. Dec 2021;44(12):2855-2856. doi:10.1007/s40618-021-01627-z
11. Gu WT, Zhou F, Xie WQ, Wang S, Yao H, Liu YT, Gao L, Wu ZB. A potential impact of SARS-CoV-2 on pituitary glands and pituitary neuroendocrine tumors. *Endocrine*. May 2021;72(2):340-348. doi:10.1007/s12020-021-02697-y
12. Shin J, Toyoda S, Nishitani S, Fukuhara A, Kita S, Otsuki M, Shimomura I. Possible Involvement of Adipose Tissue in Patients With Older Age, Obesity, and Diabetes With SARS-CoV-2 Infection (COVID-19) via GRP78 (BIP/HSPA5): Significance of Hyperinsulinemia Management in COVID-19. *Diabetes*. Dec 2021;70(12):2745-2755. doi:10.2337/db20-1094
13. Poma AM, Bonuccelli D, Giannini R, Macerola E, Vignali P, Ugolini C, Torregrossa L, Proietti A, Pistello M, Basolo A, Santini F, Toniolo A, Basolo F. COVID-19 autopsy cases: detection of virus in endocrine tissues. *J Endocrinol Invest*. Jun 30 2021:1-6. doi:10.1007/s40618-021-01628-y
14. Clarke SA, Abbara A, Dhillo WS. Impact of COVID-19 on the Endocrine System: A Mini-review. *Endocrinology*. Jan 1 2022;163(1)doi:10.1210/endocr/bqab203
15. Basolo A, Poma AM, Bonuccelli D, Proietti A, Macerola E, Ugolini C, Torregrossa L, Giannini R, Vignali P, Basolo F, Santini F, Toniolo A. Adipose tissue in COVID-19: detection of SARS-CoV-2 in adipocytes and activation of the interferon-alpha response. *J Endocrinol Invest*. Feb 15 2022:1-9. doi:10.1007/s40618-022-01742-5

16. Li D, Jin M, Bao P, Zhao W, Zhang S. Clinical Characteristics and Results of Semen Tests Among Men With Coronavirus Disease 2019. *JAMA Netw Open*. May 1 2020;3(5):e208292. doi:10.1001/jamanetworkopen.2020.8292

17. Dutta S, Sengupta P. SARS-CoV-2 and Male Infertility: Possible Multifaceted Pathology. *Reprod Sci*. Jan 2021;28(1):23-26. doi:10.1007/s43032-020-00261-z

18. Baggen J, Vanstreels E, Jansen S, Daelemans D. Cellular host factors for SARS-CoV-2 infection. *Nat Microbiol*. Oct 2021;6(10):1219-1232. doi:10.1038/s41564-021-00958-0

19. Hoffmann M, Kleine-Weber H, Schroeder S, Krüger N, Herrler T, Erichsen S, Schiergens TS, Herrler G, Wu NH, Nitsche A, Müller MA, Drosten C, Pöhlmann S. SARS-CoV-2 Cell Entry Depends on ACE2 and TMPRSS2 and Is Blocked by a Clinically Proven Protease Inhibitor. *Cell*. Apr 16 2020;181(2):271-280.e8. doi:10.1016/j.cell.2020.02.052

20. Ren X, Wang S, Chen X, Wei X, Li G, Ren S, Zhang T, Zhang X, Lu Z, You Z, Wang Z, Song N, Qin C. Multiple Expression Assessments of ACE2 and TMPRSS2 SARS-CoV-2 Entry Molecules in the Urinary Tract and Their Associations with Clinical Manifestations of COVID-19. *Infect Drug Resist*. 2020;13:3977-3990. doi:10.2147/idr.S270543

21. Wang W, Xu Y, Gao R, Lu R, Han K, Wu G, Tan W. Detection of SARS-CoV-2 in Different Types of Clinical Specimens. *Jama*. May 12 2020;323(18):1843-1844. doi:10.1001/jama.2020.3786

22. Edenfield RC, Easley CAt. Implications of testicular ACE2 and the renin-angiotensin system for SARS-CoV-2 on testis function. *Nat Rev Urol*. Feb 2022;19(2):116-127. doi:10.1038/s41585-021-00542-5

23. Mruk DD, Cheng CY. The Mammalian Blood-Testis Barrier: Its Biology and Regulation. *Endocr Rev*. Oct 2015;36(5):564-91. doi:10.1210/er.2014-1101

24. Qu N, Ogawa Y, Kuramasu M, Nagahori K, Sakabe K, Itoh M. Immunological microenvironment in the testis. *Reprod Med Biol*. Jan 2020;19(1):24-31. doi:10.1002/rmb2.12293

25. Abbasi AZ, Kiyani DA, Hamid SM, Saalim M, Fahim A, Jalal N. Spiking dependence of SARS-CoV-2 pathogenicity on TMPRSS2. *J Med Virol*. Jul 2021;93(7):4205-4218. doi:10.1002/jmv.26911

26. Erbay G, Sanli A, Turel H, Yavuz U, Erdogan A, Karabakan M, Yaris M, Gultekin MH. Short-term effects of COVID-19 on semen parameters: A multicenter study of 69 cases. *Andrology*. Jul 2021;9(4):1060-1065. doi:10.1111/andr.13019

27. Song C, Wang Y, Li W, Hu B, Chen G, Xia P, Wang W, Li C, Diao F, Hu Z, Yang X, Yao B, Liu Y. Absence of 2019 novel coronavirus in semen and testes of COVID-19 patients†. *Biol Reprod*. Jun 23 2020;103(1):4-6. doi:10.1093/biolre/ioaa050

28. Ma X, Guan C, Chen R, Wang Y, Feng S, Wang R, Qu G, Zhao S, Wang F, Wang X, Zhang D, Liu L, Liao A, Yuan S. Pathological and molecular examinations of postmortem testis biopsies reveal SARS-CoV-2 infection in the testis and spermatogenesis damage in COVID-19 patients. *Cell Mol Immunol*. Feb 2021;18(2):487-489. doi:10.1038/s41423-020-00604-5

29. Salciccia S, Del Giudice F, Gentile V, Mastroianni CM, Pasculli P, Di Lascio G, Ciardi MR, Sperduti I, Maggi M, De Berardinis E, Eisenberg ML, Sciarra A. Interplay between male testosterone levels and the risk for subsequent invasive respiratory assistance among COVID-19 patients at hospital admission. *Endocrine*. Nov 2020;70(2):206-210. doi:10.1007/s12020-020-02515-x

30. Rastrelli G, Di Stasi V, Inglese F, Beccaria M, Garuti M, Di Costanzo D, Spreafico F, Greco GF, Cervi G, Pecoriello A, Magini A, Todisco T, Cipriani S, Maseroli E, Corona G, Salonia A, Lenzi A, Maggi M, De Donno G, Vignozzi L. Low testosterone levels predict clinical adverse outcomes in SARS-CoV-2 pneumonia patients. *Andrology*. Jan 2021;9(1):88-98. doi:10.1111/andr.12821

31. Johnson L, Petty CS, Neaves WB. Influence of age on sperm production and testicular weights in men. *J Reprod Fertil*. Jan 1984;70(1):211-8. doi:10.1530/jrf.0.0700211

32. Johnson L, Barnard JJ, Rodriguez L, Smith EC, Swerdloff RS, Wang XH, Wang C. Ethnic differences in testicular structure and spermatogenic potential may predispose testes of Asian men to a heightened sensitivity to steroidal contraceptives. *J Androl*. May-Jun 1998;19(3):348-57.

33. Loibner M, Langner C, Regitnig P, Gorkiewicz G, Zatloukal K. Biosafety Requirements for Autopsies of Patients with COVID-19: Example of a BSL-3 Autopsy Facility Designed for Highly Pathogenic Agents. *Pathobiology*. 2021;88(1):37-45. doi:10.1159/000513438

34. Heller C, Heller G, Rowley M. Human spermatogenesis: an estimate of the duration of each cell association and of each cell type. *Excerpta Medica Inter Cong Ser*. 1969;184:1012-1018.

35. Cassella L, Salvetti A, Iacopetti P, Ippolito C, Ghezzani C, Gimenez G, Ghigo E, Rossi L. Putrescine independent wound response phenotype is produced by ODC-like RNAi in planarians. *Sci Rep*. Aug 29 2017;7(1):9736. doi:10.1038/s41598-017-09567-6

36. Handelsman DJ, Staraj S. Testicular size: the effects of aging, malnutrition, and illness. *J Androl*. May-Jun 1985;6(3):144-51. doi:10.1002/j.1939-4640.1985.tb00830.x

37. Jackson CB, Farzan M, Chen B, Choe H. Mechanisms of SARS-CoV-2 entry into cells. *Nat Rev Mol Cell Biol*. Jan 2022;23(1):3-20. doi:10.1038/s41580-021-00418-x

38. Shen Q, Xiao X, Aierken A, Yue W, Wu X, Liao M, Hua J. The ACE2 expression in Sertoli cells and germ cells may cause male reproductive disorder after SARS-CoV-2 infection. *J Cell Mol Med*. Aug 2020;24(16):9472-9477. doi:10.1111/jcmm.15541

39. Al-Benna S. Association of high level gene expression of ACE2 in adipose tissue with mortality of COVID-19 infection in obese patients. *Obes Med*. Sep 2020;19:100283. doi:10.1016/j.obmed.2020.100283

40. Mäkelä JA, Koskenniemi JJ, Virtanen HE, Toppari J. Testis Development. *Endocr Rev*. Aug 1 2019;40(4):857-905. doi:10.1210/er.2018-00140

41. McEwan IJ, Brinkmann AO. Androgen Physiology: Receptor and Metabolic Disorders. In: Feingold KR, Anawalt B, Boyce A, et al, eds. *Endotext*. MDText.com, Inc.

Copyright © 2000-2022, MDText.com, Inc.; 2000.

42. Poma AM, Proietti A, Macerola E, Bonuccelli D, Conti M, Salvetti A, Dolo V, Chillà A, Basolo A, Santini F, Toniolo A, Basolo F. Suppression of pituitary hormone genes in subjects who died from COVID-19 independently of virus detection in the gland. *J Clin Endocrinol Metab*. May 14 2022;doi:10.1210/clinem/dgac312

43. Richardson RB, Ohlson MB, Eitson JL, Kumar A, McDougal MB, Boys IN, Mar KB, De La Cruz-Rivera PC, Douglas C, Konopka G, Xing C, Schoggins JW. A CRISPR screen identifies IFI6 as an ER-resident interferon effector that blocks flavivirus replication. *Nat Microbiol*. Nov 2018;3(11):1214-1223. doi:10.1038/s41564-018-0244-1

44. Dukhovny A, Lamkiewicz K, Chen Q, Fricke M, Jabrane-Ferrat N, Marz M, Jung JU, Sklan EH. A CRISPR Activation Screen Identifies Genes That Protect against Zika Virus Infection. *J Virol*. Aug 15 2019;93(16)doi:10.1128/jvi.00211-19

45. Liu C, Boland S, Scholle MD, Bardiot D, Marchand A, Chaltin P, Blatt LM, Beigelman L, Symons JA, Raboisson P, Gurard-Levin ZA, Vandyck K, Deval J. Dual inhibition of SARS-CoV-2 and human rhinovirus with protease inhibitors in clinical development. *Antiviral Res*. Mar 2021;187:105020. doi:10.1016/j.antiviral.2021.105020

46. Perng YC, Lenschow DJ. ISG15 in antiviral immunity and beyond. *Nat Rev Microbiol*. Jul 2018;16(7):423-439. doi:10.1038/s41579-018-0020-5

47. Li H, Fu YX, Wu Q, Zhou Y, Crossman DK, Yang P, Li J, Luo B, Morel LM, Kabarowski JH, Yagita H, Ware CF, Hsu HC, Mountz JD. Interferon-induced mechanosensing defects impede apoptotic cell clearance in lupus. *J Clin Invest*. Jul 1 2015;125(7):2877-90. doi:10.1172/jci81059

48. Afshin A, Forouzanfar MH, Reitsma MB, Sur P, Estep K, Lee A, Marczak L, Mokdad AH, Moradi-Lakeh M, Naghavi M, Salama JS, Vos T, Abate KH, Abbafati C, Ahmed MB, Al-Aly Z, Alkerwi A, Al-Raddadi R, Amare AT, Amberbir A, Amegah AK, Amini E, Amrock SM, Anjana RM, Ärnlöv J, Asayesh H, Banerjee A, Barac A, Baye E, Bennett DA, Beyene AS, Biadgilign S, Biryukov S, Bjertness E, Boneya DJ, Campos-Nonato I, Carrero JJ, Cecilio P, Cercy K, Ciobanu LG, Cornaby L, Damtew SA, Dandona L, Dandona R, Dharmaratne SD, Duncan BB, Eshrati B, Esteghamati A, Feigin VL, Fernandes JC, Fürst T, Gebrehiwot TT, Gold A, Gona PN, Goto A, Habtewold TD,

Hadush KT, Hafezi-Nejad N, Hay SI, Horino M, Islami F, Kamal R, Kasaeian A, Katikireddi SV, Kengne AP, Kesavachandran CN, Khader YS, Khang YH, Khubchandani J, Kim D, Kim YJ, Kinfu Y, Kosen S, Ku T, Defo BK, Kumar GA, Larson HJ, Leinsalu M, Liang X, Lim SS, Liu P, Lopez AD, Lozano R, Majeed A, Malekzadeh R, Malta DC, Mazidi M, McAlinden C, McGarvey ST, Mengistu DT, Mensah GA, Mensink GBM, Mezgebe HB, Mirrakhimov EM, Mueller UO, Noubiap JJ, Obermeyer CM, Ogbo FA, Owolabi MO, Patton GC, Pourmalek F, Qorbani M, Rafay A, Rai RK, Ranabhat CL, Reinig N, Safiri S, Salomon JA, Sanabria JR, Santos IS, Sartorius B, Sawhney M, Schmidhuber J, Schutte AE, Schmidt MI, Sepanlou SG, Shamsizadeh M, Sheikhbahaei S, Shin MJ, Shiri R, Shiue I, Roba HS, Silva DAS, Silverberg JI, Singh JA, Stranges S, Swaminathan S, Tabarés-Seisdedos R, Tadese F, Tedla BA, Tegegne BS, Terkawi AS, Thakur JS, Tonelli M, Topor-Madry R, Tyrovolas S, Ukwaja KN, Uthman OA, Vaezghasemi M, Vasankari T, Vlassov VV, Vollset SE, Weiderpass E, Werdecker A, Wesana J, Westerman R, Yano Y, Yonemoto N, Yonga G, Zaidi Z, Zenebe ZM, Zipkin B, Murray CJL. Health Effects of Overweight and Obesity in 195 Countries over 25 Years. *N Engl J Med*. Jul 6 2017;377(1):13-27. doi:10.1056/NEJMoa1614362

49. Weider T, Genoni A, Broccolo F, Paulsen T, Dahl-Jorgensen K, Toniolo A, Hammerstad SS. High Prevalence of Common Human Viruses in Thyroid Tissue. *Frontiers in Endocrinology*. 2022:1582. doi:https://doi.org/10.3389/fendo.2022.938633

50. Alfano M, Tascini AS, Pederzoli F, Locatelli I, Nebuloni M, Giannese F, Garcia-Manteiga JM, Tonon G, Amodio G, Gregori S, Agresti A, Montorsi F, Salonia A. Aging, inflammation and DNA damage in the somatic testicular niche with idiopathic germ cell aplasia. *Nat Commun*. Sep 1 2021;12(1):5205. doi:10.1038/s41467-021-25544-0

51. Wu H, Jiang X, Gao Y, Liu W, Wang F, Gong M, Chen R, Yu X, Zhang W, Gao B, Song C, Han D. Mumps virus infection disrupts blood-testis barrier through the induction of TNF-α in Sertoli cells. *Faseb j*. Nov 2019;33(11):12528-12540. doi:10.1096/fj.201901089R

52. Griffin DE. Why does viral RNA sometimes persist after recovery from acute infections? *PLoS Biol*. Jun 2022;20(6):e3001687. doi:10.1371/journal.pbio.3001687

Figures legends

Figure 1. Histopathology and immunostaining of testis specimen of COVID-19 autopsy cases

A) Hematoxylin and eosin staining: well-preserved seminiferous tubuli in a COVID-19 case (original magnification 10X, scale bar 100 µm). B) Spike RNA genome/transcripts of SARS-CoV-2 revealed by in situ hybridization in testis of a COVID-19 case. Brown granuli are detected more frequently in Leydig cells (black arrow; original magnification 60X, scale bar 50 µm). C) Granular brown staining for the SARS-CoV-2 nucleocapsid (N) antigen distributed mainly in cells of the extra-tubular space (original magnification 60X, scale bar 50 µm). D) CD8 T-cells scattered among seminiferous tubuli (original magnification 20X, scale bar 50 µm). E) Cluster of CD68 macrophages in the extra-tubular space (original magnification 20X, scale bar 100 µm). F) Brown nuclear staining for the androgen receptor in several cells of seminiferous tubuli (original magnification 40X, scale bar 50 µm). G)

Prevalent brown cell membrane staining for the FSH receptor in cells of seminiferous tubuli (original magnification 40X, scale bar 50 µm). H) Expression of the LHCG receptor in a COVID-19 case that was virus-positive in testis tissue: diffuse brown staining of cells in the extra-tubular space (original magnification 20X, scale bar 100 µm).

Figure 2. Transmission electron microscopy of testicle tissue from a 73 years-old COVID-19 subject. A) Micrograph showing the lamina propria of testis. Arrows indicate longitudinal and cross section collagen fibers. The arrowhead indicates a vesicle surrounded by membrane containing virus-like particles. n: nucleus. Scale bar, 1 µm. B) Higher magnification of the vesicle in A. Virus-like particles showing the envelope membrane and faint projections on their surface. Scale bar, 200 nm.

Figure 3. Correlation between immune cell counts and transcription levels of testis-specific genes. Immune cell counts were positively correlated among themselves. The same occurred for transcripts levels of testis-specific genes. In contrast, levels of infiltrating immune cells were negatively related to selected testis-specific transcripts (ADAD1, ADAM2, H2AC1, H2BC1, SLC25A31, TUBA3C). Transcription of genes mostly expressed in spermatidis (ACTL7B, CCDC70, HMGB4, LYZL1, SUN5, TEX33) was reduced but not related to immune cell counts. Shades of blue, degree of positive correlation,; shades of red, degree of negative correlation. Non-significant correlations are marked with X.

Figure 4. Immunohistochemical expression of reproductive hormone receptors in testicle tissue of COVID-19 cases and controls. Expression of androgen receptor (AR), and follicle stimulating hormone receptor (FSHR) in seminiferous tubuli. Expression of luteinizing hormone/choriogonadotropin receptor (LHCGR) in extra-tubular cells. Mean percentages of stained cells ± S.D. are presented. Asterisks indicate statistically significant results (p<0.05).

Tables

Table 1. Demographic and clinical characteristics of autopsy cases

	Control subjects (n=10)	**COVID-19 subjects (n=24)**	
	SARS-CoV-2 negative (n=10)	**SARS-CoV-2 negative in testes (n=15)**	**SARS-CoV-2 positive in testes (n=9)**
Detection of SARS-CoV-2 by RT-PCR			
Lungs	negative	positive	positive
Testis	negative	negative	positive
Age			
years, median (range)	63.5 (20-81)	70 (41-85)	73 (39-89)
BMI[1]			
kg/m^2, median (IQR[2])	23.7 (22.2-24.0)	25.7 (23.6-27.7) *	26.1 (23.7-32.3) *
Previous diseases			
Cardiovascular disease	4 (40%)	8 (53%)	5 (56%)
Chronic pulmonary disease	0	1 (7%)	1 (11%)
Diabetes	0	2 (13%)	4 (44%)
Malignancy	2 (20%)	2 (13%)	0
Severe kidney	1 (10%)	0	2 (22%)

impairment[1]			
Neurological disease	1 (10%)	0	0
Received a COVID-19 vaccine			
single shot	0	0	1 (11%)
two or more shots	2 (20%)	3 (20%)	2 (22%)
Respiratory support			
Simple oxygen	0	1 (7%)	2 (22%)
Mechanical ventilation	0	10 (67%)	1 (11%)
COVID-19 treatment	NA	Non-steroidal anti-inflammatories; corticosteroids; antibacterials/antifungals; prophylactic anticoagulation or full dose heparinization. Remdesivir in some cases. As needed: inotropic drugs, inhaled bronchodilators, insulin or metformin, levothyroxine	
Days from initial symptoms to death			
median (IQR)**	NA	21 (6-27)	6 (4-7) *
Days from death to autopsy			
median (IQR[2])	3 (2-5)	1 (1-4)	4 (3-5)

1. BMI, body mass index. BMI was significantly higher in COVID-19 cases as compared to controls.
2. IQR, interquartile range.
*, the asterisk indicates a statistical difference among groups **IQR, interquartile range

Table 2. Size of testicles and counts of spermatogenic cells in uninfected control subjects and Covid-19 subjects.

	Control subjects (n=10)	COVID-19 subjects (n=24)	
	Controls (n=10)	**SARS-CoV-2 negative in testes (n=15)**	**SARS-CoV-2 positive in testes (n=9)**
Testicle size (cm)[1]			
Length	4.7 ± 0.8	4.3 ± 0.7	4.3 ± 0.5
Width	4.0 ± 0.5	3.5 ± 0.5	3.5 ± 0.4
Spermatogenic cells (numbers per 10 tubuli)[2]			
Spermatogonia	249.0± 172.7	183.4 ± 131.4	190.0 ± 85.7
Spermatocytes	278.4 ± 199.2	148.0 ± 120.2	178.0 ± 87.7
Spermatids	292.0 ± 223.2	152.3 ± 129.2	191.3 ± 90.5

1. Length and width of testicles as measured with a ruler at autopsy (mean ± SD). No statistically significant differences were found among groups using one-way Anova by Tukey test.
2. Differential counts of spermatogenic cells in H&E slides (mean ± SD). No statistically significant differences were found among groups using one-way Anova by Tukey test.

Table 3. Deregulated expression of immune-related and testis-specific genes.

Gene	**Cellular localization of transcripts**	**COVID-19 SARS-CoV-2-negative in testicles vs. control**		**COVID-19 SARS-CoV-2-positive in testicles vs. control**	
		Log2 FC	***FDR***	**Log2 FC**	***FDR***
Immune-related genes					
IFI6 (IFN-alpha Inducible Protein 6)	-	1.08	0.18	2.69	0.001*
ISG15 (Ubiquitin Like Modifier)	-	-0.14	0.86	1.99	0.14
MARCO (Macrophage Receptor With Collagenous Structure)	-	1.99	0.15	2.66	0.14
Testis-specific genes					
SLC25A31 (Solute Carrier Family 25 Member 31)	Spermatocytes Spermatidis Leydig Cells*	-0.74	0.137	-0.60	0.149
H2AC1 (H2A Clustered Histone 1)	Male germ cells	-0.49	0.422	-0.60	0.246
HMGB4 (High Mobility Group Box 4)	Spermatidis	-1.65	0.423	-1.92	0.273
ADAD1 (Adenosine Deaminase Domain Containing 1)	Spermatidis Spermatocytes	-0.39	0.487	-0.68	0.160

TUBA3C (Tubulin Alpha 3c)	Spermatocytes Spermatidis Leydig Cells* Sertoli Cells*	-0.40	0.512	-0.83	0.119
CCDC70 (Coiled-Coil Domain Containing 70)	Spermatidis	-1.09	0.552	-1.74	0.263
ACTL7B (Actin Like 7B)	Spermatidis	-0.92	0.614	-1.41	0.363
ADAM2 (ADAM Metallopeptidase Domain 2)	Spermatocytes Spermatidis Leydig Cells*	-0.33	0.676	-0.59	0.382
SUN5 (Testis And Spermatogenesis Related Gene 4)	Spermatidis	-0.59	0.687	-1.03	0.410
H2BC1 (Testis-Specific Histone H2B)	Male germ cells	-0.24	0.719	-0.59	0.289
TEX33 (Testis Expressed 33)	Spermatidis Sertoli Cells*	-0.25	0.772	-1.16	0.118
LYZL1 (Lysozyme Like 1)	Spermatidis Spermatocytes Sertoli Cells* Leydig Cells*	-0.12	0.887	-0.76	0.634

*, Low-level expression according to the The Human Protein Atlas (https://www.proteinatlas.org/)

Table 4. Significantly deregulated gene pathways.

Gene set	ID	Set size	NES	FDR
Virus-positive testis of COVID-19 cohort *vs* controls				
Hallmark collection				
HALLMARK_INTERFERON_GAMMA_RESPONSE	M5913	87	1.61	0.000006
HALLMARK_INTERFERON_ALPHA_RESPONSE	M5911	45	1.62	0.0003
HALLMARK_TNFA_SIGNALING_VIA_NFKB	M5890	62	1.45	0.007
HALLMARK_COMPLEMENT	M5921	43	1.45	0.017
HALLMARK_INFLAMMATORY_RESPONSE	M5932	62	1.37	0.038
Gene Ontology collection				
Gene Ontology and Biological Pathways (GOBP) DEFENSE_RESPONSE	GO:0006952	298	1.42	0.003
GOBP_DEFENSE_RESPONSE_TO_OTHER_ORGANISM	GO:0098542	224	1.41	0.003
GOBP_RESPONSE_TO_BIOTIC_STIMULUS	GO:0009607	274	1.40	0.003
GOBP_RESPONSE_TO_INTERFERON_GAMMA	GO:0034341	71	1.56	0.008
GOBP_INNATE_IMMUNE_RESPONSE	GO:0045087	194	1.39	0.017
GOBP_RESPONSE_TO_TYPE_I_INTERFERON	GO:0034340	47	1.58	0.038
GOBP_VIRAL_GENOME_REPLICATION	GO:0019079	26	1.66	0.042
Virus-negative testis of COVID-19 cohort *vs* controls				
Hallmark collection				
HALLMARK_INFLAMMATORY_RESPONSE	M5932	62	1.56	0.024
HALLMARK_ALLOGRAFT_REJECTION	M5950	67	1.51	0.032
Gene Ontology collection				
None	N.A.	N.A.	N.A.	N.A.

FDR, false discovery rate

NES, normalized enriched score

N.A., not applicable.

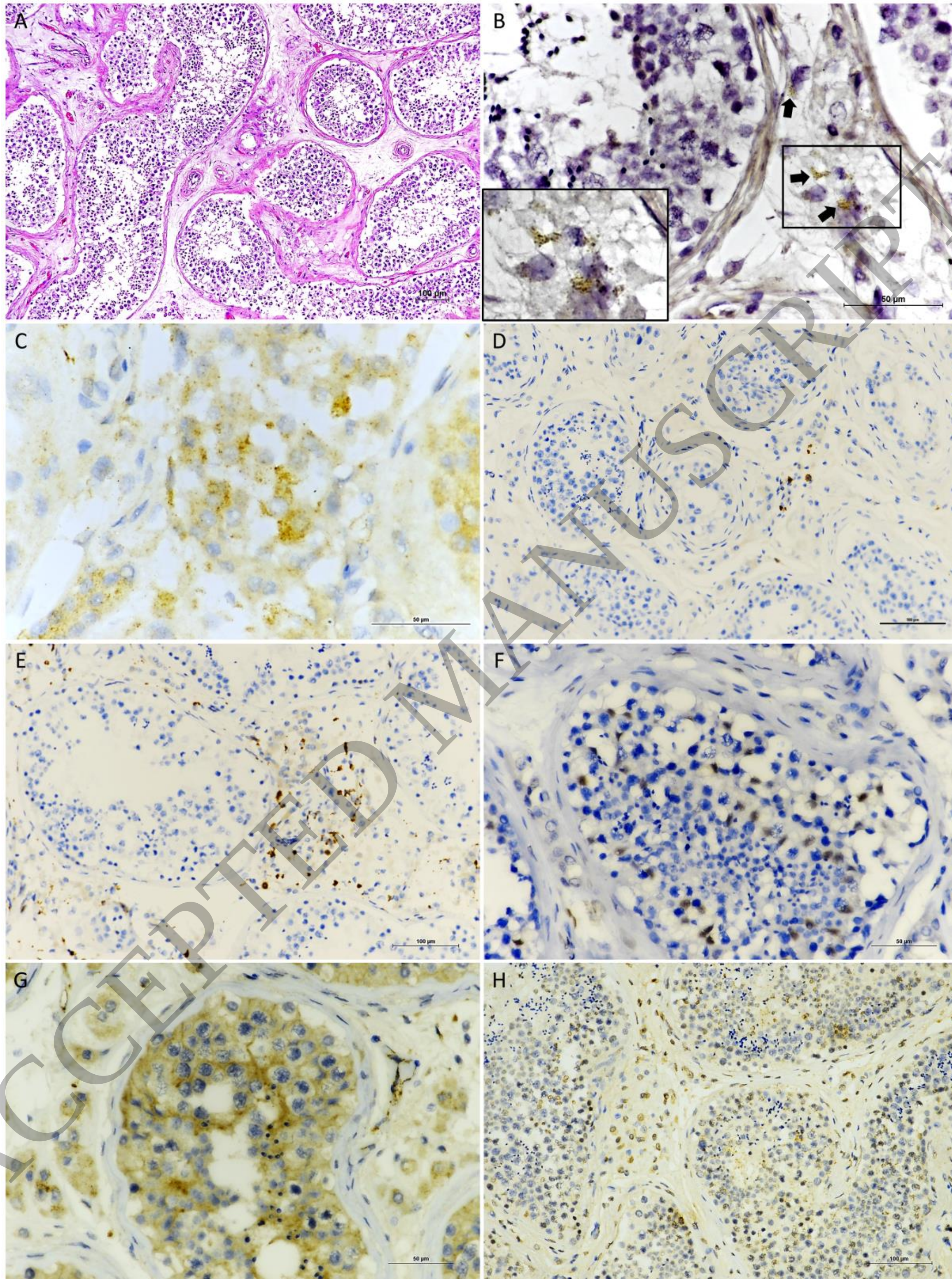

Figure 1
154x205 mm (0.3 x DPI)

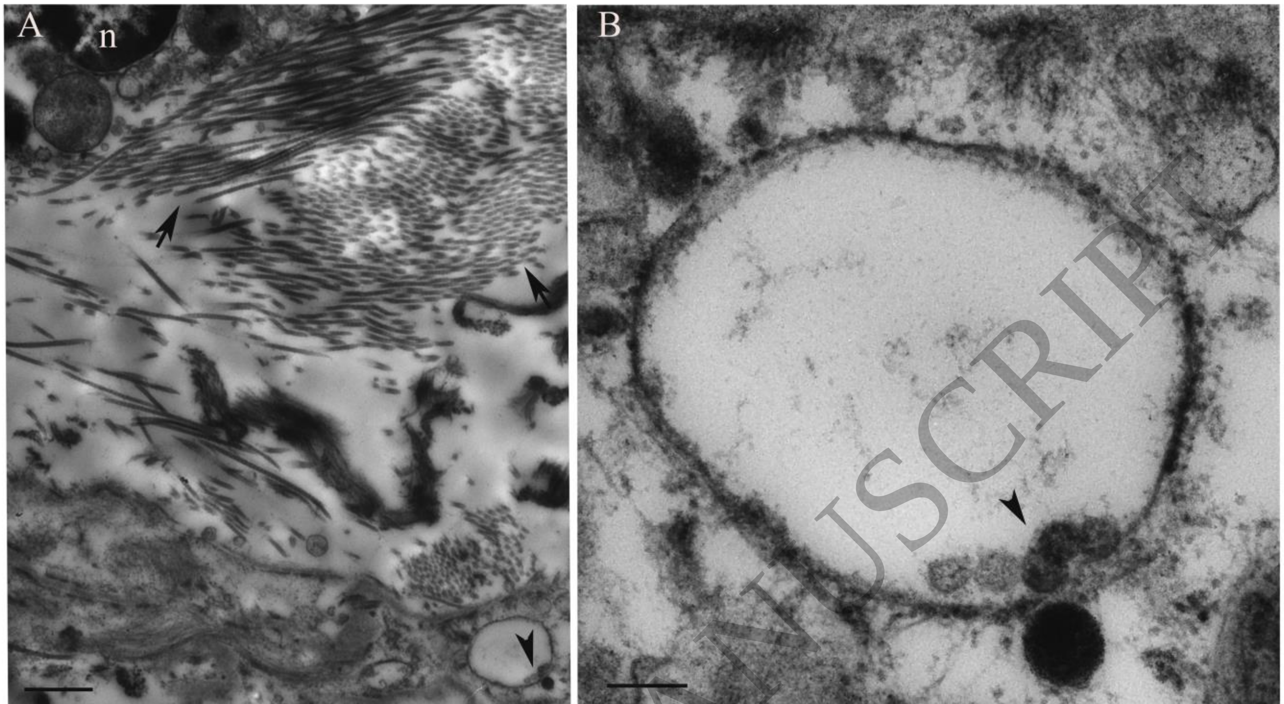

Figure 2
180x110 mm (0.3 x DPI)

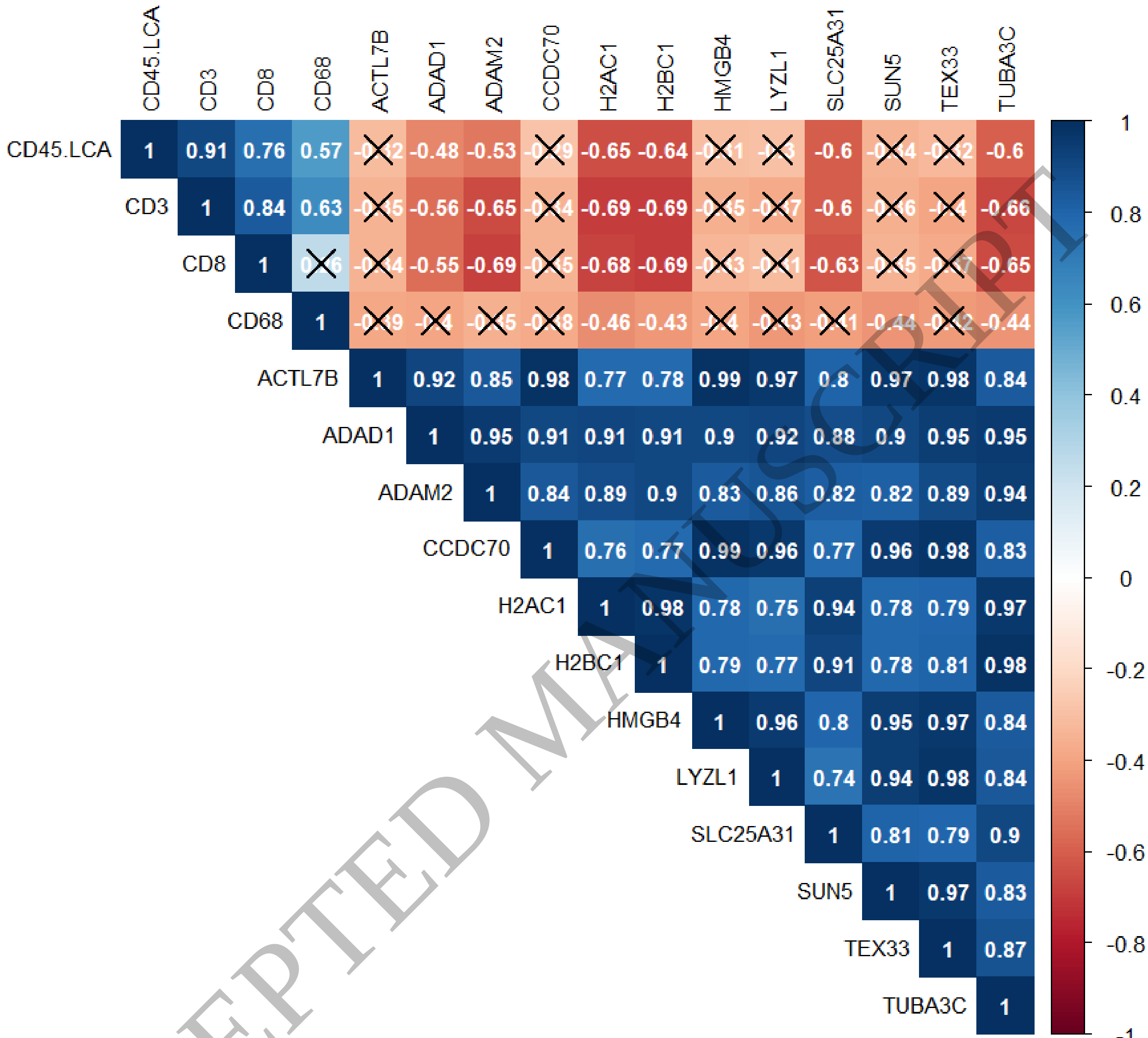

Figure 3
302x276 mm (0.3 x DPI)

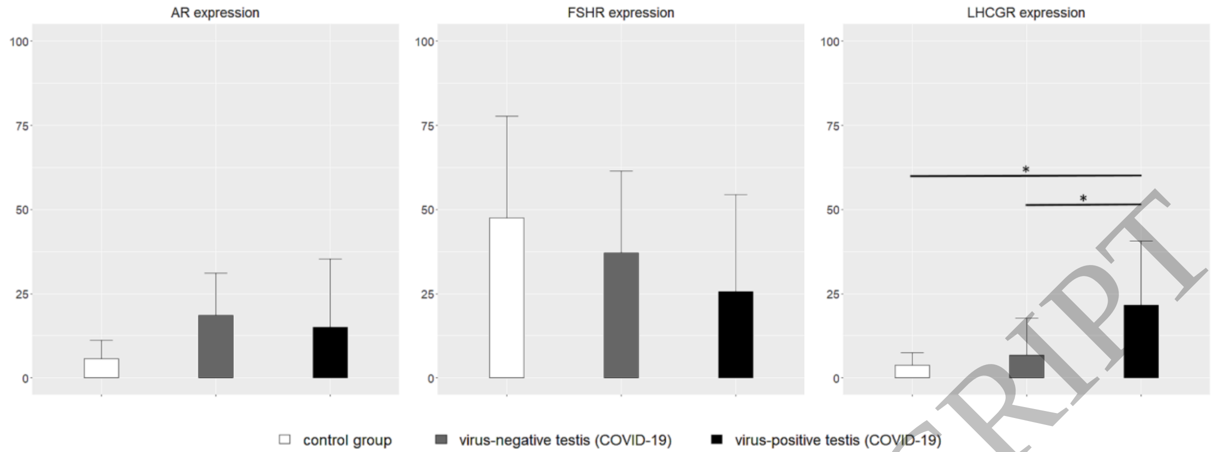

Figure 4
160x62 mm (0.3 x DPI)